Materials Research. 2015; 18(Suppl 2): 138-142
DOI: http://dx.doi.org/10.1590/1516-1439.352114

Effect of Cooling Rate on the Corrosion Behavior of As-Cast SAF 2205 Duplex Stainless Steel After Solution Annealing Treatment

Maria Eurenice Rocha Cronemberger[a]*, Sandra Nakamatsu[b], Carlos Alberto Della Rovere[a], Sebastião Elias Kuri[a], Neide Aparecida Mariano[b]

[a]Programa de Pós-Graduação em Ciência e Engenharia de Materiais – PPG-CEM, Universidade Federal de São Carlos – UFSCar, Rod. Washington Luís, Km 235, SP-310, São Carlos, SP, Brazil
[b]Programa de Pós-Graduação em Ciência e Engenharia de Materiais – PPG-CEM, Universidade Federal de Alfenas – UNIFAL-MG, Rod. José Aurélio Vilela, 11999, Poços de Caldas, MG, Brazil

Received: November 12, 2014; Revised: June 12, 2015

The formation of intermetallic phases alters the properties of duplex stainless steel and is therefore a crucial factor in its performance. For example, the formation of sigma phase in duplex steel increases its brittleness and decreases its corrosion resistance because this phase consumes chromium and molybdenum in solid solution, thus leading to the depletion of these elements in the matrix. This study investigated the corrosion resistance of as-cast SAF 2205 duplex stainless steel after solution annealing treatment at 1100 °C for 240 minutes, under varying cooling rates. The objective was to evaluate the correlation between cooling condition, microstructural changes and corrosion resistance based on cyclic potentiodynamic polarization and double loop electrochemical potentiokinetic reactivation (DL-EPR) measurements. The results revealed a significant reduction in the corrosion resistance of a slowly cooled sample, which presented an increase in the degree of Cr (Qr / Qa) depletion resulting from the formation of sigma phase.

Keywords: *duplex stainless steel, corrosion, solution annealing, cooling conditions*

1. Introduction

The addition of large amounts of alloying elements may cause the microstructure of duplex stainless steels to become unstable, and precipitation of intermetallic phases may occur during solidification, heat treatment, welding processes, or by thermal aging, if these processes are not carefully controlled[1-4]. The presence of these phases, such as $M_{23}C_6$ carbide, chromium nitride, chi, sigma and alpha prime, deteriorates the properties of steel due to the uneven distribution of alloying elements and their depletion in adjacent regions[1,2,5,6]. The formation of sigma (Cr-rich phase) through ferrite phase decomposition, for example, usually causes Cr depletion in underlying regions, making them more susceptible to corrosion[4,5,7]. As for corrosion resistance, electrochemical techniques are extensively used to evaluate the corrosion behavior of stainless steels.

The main corrosion parameters can be determined based on cyclic potentiodynamic polarization (CPP). On the other hand, the influence of the precipitation of intermetallic phases on the corrosion resistance of stainless steels can be evaluated based on double loop – electrochemical potentiokinetic reactivation (DL-EPR) tests, which provide information about chromium depletion[8,9].

The effects of the solution annealing treatment temperature and also of isothermal aging conditions on the precipitation of secondary phases have been discussed extensively[1,3,6,10-13], but few investigations have focused on their formation during continuous cooling after solution treatment, when processed differently[14,15]. The cooling rate is an important parameter that can affect time and temperature during exposure of the material to heat treatment or under working conditions. During slow cooling, some newly formed phases may continue to develop or other transformations may occur when lower temperatures are exceeded.

This study investigated the effects of different cooling rates on microstructure and corrosion resistance of SAF 2205 duplex stainless steel (2205 DSS) solution annealing treated from the as-cast condition, through X-ray diffraction, optical microscopy and electrochemical tests.

2. Experimental Procedure

Steel samples were solution annealing treated at a temperature of 1100 °C for 240 minutes[1,15,16], and each one was cooled differently: in water (rapid cooling), air (moderate) or furnace (slow). Microstructural modifications were investigated by optical microscopy (OM) and X-ray diffraction analyses (XRD), performed on AXS Analytical X-Ray Systems Siemens D5005 diffractometer using Cu radiation Kα with range scanning of $5\,° \leq 2\theta \leq 90\,°$ and step of 0.033 °/s. The samples were prepared according to the ASTM E3-11[17] standard and etched according to the ASTM E407-07e1[18] standard, using Beraha's reagent [composed of 10 mL hydrochloric acid (HCl), 90 mL distilled water and 1 g potassium metabisulfite ($K_2S_2O_5$)].

*e-mail: mariaeurenice@gmail.com

For the electrochemical measurements, the samples were embedded in polyester resin after establishing the electrical contact, taking special care to prevent the formation of crevices. A conventional three-electrode electrochemical cell was used with a platinum counter electrode and a saturated calomel reference electrode (SCE) connected to a Metrohm potentiostat, Autolab/PGSTART302. To ensure good reproducibility, a minimum of three sets of measurements of each sample were taken and an average value was considered.

CPP tests were performed according to ASTM G5-94[19], in a naturally aerated synthetic marine solution of 60,000 mg/L Cl^- at room temperature, which was prepared according to ASTM D1141-98[20]. After immersion, the samples were subjected to open circuit conditions for 30 minutes, until reached a steady-state potential, considering this the open-circuit potential (E_{OC}). The scans were performed at sweep rates of 1 mV/s, starting from a potential of 200 mV below E_{OC} to a potential at which the current density reached 1 mA/cm^2, from which the scan was changed to cathodic direction[21].

The DL-EPR measurements were carried out in a solution of 0.5 M H2SO4 + 0.001 M thioacetamide (TA) at 60 °C[22,23]. The potential scan was started 5 minutes after samples immersion, initially in the anodic direction from –500 mV(SCE) to 300 mV(SCE), and after reversed to the cathodic direction up to –500 mV(SCE), with 1.67 mV/s scan rate. The degree of Cr depletion was evaluated in terms of the charges ratio, Qr/Qa x 100, in combination with microstructure observation by OM after the measurements. The Qa term was obtained from the polarization curve in anodic direction which is associated with sample surface charges, while Qr term is associated with Cr depleted regions susceptible to corrosion and its value was obtained from the polarization curve in the cathodic direction[24].

3. Results and Discussion

Figure 1 shows optical micrographs of solution-treated samples of 2205 DSS (22Cr 5Ni 3Mo) subjected to rapid, moderate and slow cooling rates. In this figure, note the elongated islands of austenite grains embedded in the continuous ferrite matrix and precipitated at grain boundaries.

A more homogeneously distributed microstructure and a higher volume fraction of austenite phase can apparently be obtained by decreasing the cooling rate. However, the slow cooling rate favored the precipitation of sigma phase, evidenced by XRD, shown in Figure 2.

Table 1 describes the values of the electrochemical parameters obtained from the cyclic potentiodynamic polarization curves depicted in Figure 3a. These curves were superimposed to facilitate their comparison. The E_p was taken as the potential at which a sudden sharp rise in current density occurred and the value of 100 µA/cm^2 was exceeded[25,26].

Samples cooled moderately and rapidly (in water and air, respectively) showed no significant variations in corrosion (E_c) and pitting (E_p) potentials. However, the protection potential of the moderately cooled sample was about 80% lower, indicating that the repassivation process

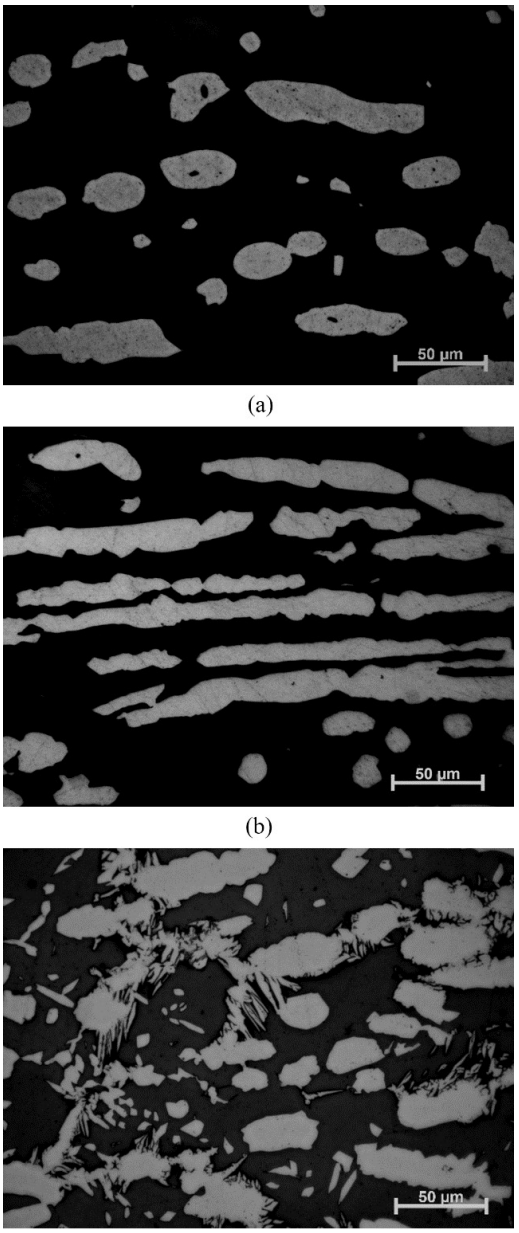

Figure 1. Optical Micrographs of 2205 DSS solution-treated and cooled (a) rapidly, (b) moderately and (c) slowly.

Table 1. Electrochemical parameters of 2205 DSS solution-treated, obtained in synthetic marine solution (60,000 mg/L de Cl-).

Treatment time/cooling	E_c [V]	E_p [V]	E_{prot} [V]
240 min/rapid	–0.2513 ± 0.02	1.1147 ± 0.01	0.9944 ± 0.01
240 min/moderate	–0.3080 ± 0.02	1.0808 ± 0.06	–0.2054 ± 0.04
240 min/slow	–0.5247 ± 0.10	0.1361 ± 0.02	–0.1982 ± 0.05

was more difficult, probably due to the formation of small depleted regions, which may have favored the instantaneous process of pitting nucleation and repassivation. This can be explained by the variations in volume fraction of ferrite and austenite phases[9] obtained for this sample (demonstrated in a previous work[16]).

On the other hand, the sample cooled slowly presented lower values of corrosion, pitting and protection potential. In this case, passivity breakdown occurred at a much lower potential than in the other samples. This limited passivity and the decrease in corrosion and protection potential can be attributed to sigma phase precipitation, which is illustrated in the diffractogram in Figure 2. The presence of sigma phase (σ) is visible only in the diffractogram of the sample subjected to a slow cooling rate.

Note an intermediary behavior of moderately cooled sample between the two others samples. While its anodic features were similar to rapidly cooled sample, in the cathodic potential scan, this sample demonstrated corrosion susceptibility, suggesting that this cooling rate could be considered limitary to precipitation of intermetallic components.

Figure 3b depicts the DL-EPR curves, which show the formation of two distinct peaks, a behavior that is considered a sign of selective corrosion between ferrite and austenite

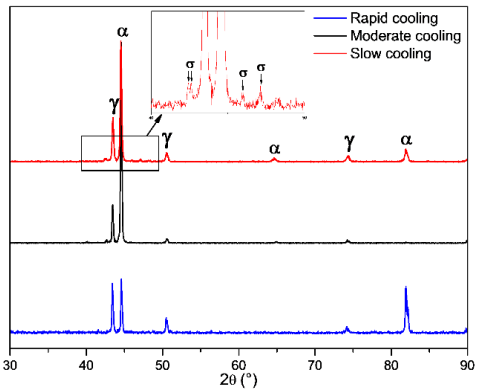

Figure 2. XRD spectra of 2205 DSS cooled rapidly, moderately and slowly.

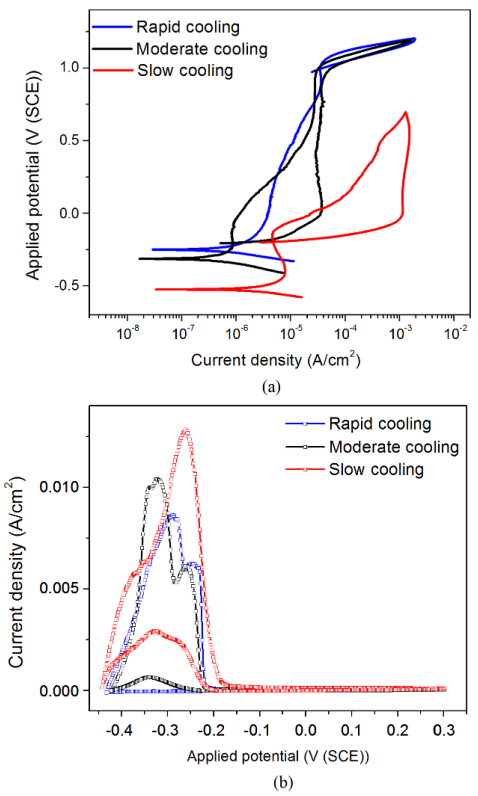

Figure 3. CPP (a) and DL-EPR (b) curves of 2205 DSS solution-treated and cooled under different conditions.

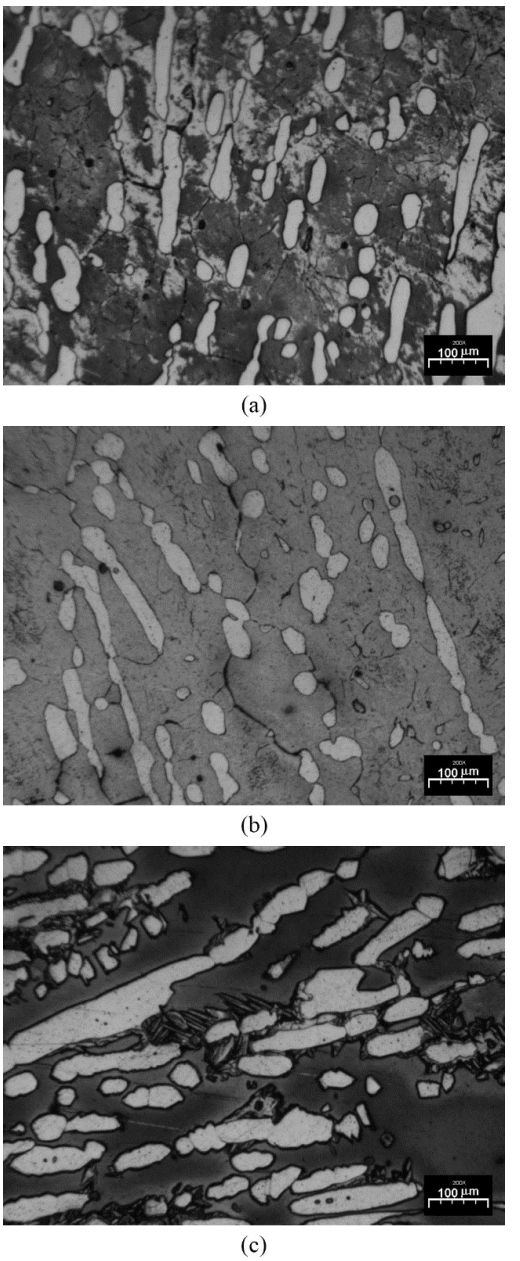

Figure 4. Optical micrographs of the surface aspect of 2205 DSS solution-treated and cooled (a) rapidly (b) moderately and (c) slowly, after DL-EPR tests.

phases[27]. Therefore, the areas under the curves were considered in the evaluation of the degree of Cr depletion in the samples, in view of the presence of two current density maxima.

Note that the reactivation current density peak was clearly absent from the solution-treated sample cooled rapidly (in water), indicating that in this condition the material was not sensitized, since the degree of Cr depletion was very limited, presenting a reduced Qr to Qa ratio (0.5 ± 0.1)[28]. This result suggests the presence of residual values inherent to the software and unavoidable deviations due to noises during measurements. Furthermore, the moderately cooled sample (air) showed a discrete reactivation current density peak, while the slowly cooled sample showed a stronger peak. The degree of Cr depletion between these samples increased from (7.1±1.0) to (26.7±2.9), indicating the formation Cr-depleted regions caused by the formation of sigma phase, which is highly deleterious to the corrosion resistance of steel, how could be also noted on cyclic polarization results.

Figure 4 shows optical micrographs of the surface of samples after the DL-EPR tests. Note that no significant attack of the ferrite phase is visible in the rapidly cooled sample, confirming the absence of Cr-depleted regions. In contrast, the moderately cooled sample shows signs of attack at the ferrite grain boundaries, which explains the slight increase in the degree of Cr depletion observed in this sample, probable caused by the decrease of its protection potential. In addition, the slowly cooled sample showed a strong attack inside the grains of the ferrite phase and at the ferrite/austenite interface, indicating that these regions are Cr-depleted. None of the samples showed any visible dissolution of the austenite phase. Sigma phase formation occurs primarily at ferrite/austenite interfaces and/or ferrite grain boundaries[2,29]; hence, sensitization of the steel occurs mainly in these regions.

This preferential attack could be explained by the higher diffusion rate of the ferrite phase and its higher Cr content, a typical site of sigma precipitation, which occurs between 600 °C and 1000 °C, through a eutectoid transformation of ferrite into austenite and sigma phase[29].

4. Conclusion

The cooling rate used after the solution annealing treatment affects the corrosion resistance of 2205 DSS. The susceptibility to corrosion of this steel increases as the cooling rate decreases, due to the formation of Cr-depleted regions. The precipitation of sigma phase, whose kinetics is favored by slow cooling, causes a considerable increase in the degree of Cr depletion inside the ferrite grain and at the ferrite/austenite interface.

Acknowledgements

The authors acknowledge to CAPES, CNPq, FAPEMIG and FAPESP.

References

1. Kashiwar A, Vennela NP, Kamath SL and Khatirkar RK. Effect of solution annealing temperature on precipitation in 2205 duplex stainless steel. *Materials Characterization*. 2012; 74:55-63. http://dx.doi.org/10.1016/j.matchar.2012.09.008.
2. Escriba DM, Materna-Morris E, Plaut RL and Padilha AF. Intermetallic phase precipitation in duplex stainless steels during high temperature exposition. *Materials Science Forum*. 2010; 636-637:478-484. http://dx.doi.org/10.4028/www.scientific.net/MSF.636-637.478.
3. Gholami M, Hoseinpoor M and Moayed MH. A statistical study on the effect of annealing temperature on pitting corrosion resistance of 2205 duplex stainless steel. *Corrosion Science*. 2015; 94:156-164. http://dx.doi.org/10.1016/j.corsci.2015.01.054.
4. Leiva-García R, Fernandes JCS, Muñoz-Portero MJ and García-Antón J. Study of the sensitisation process of a duplex stainless steel (UNS 1.4462) by means of confocal microscopy and localised electrochemical techniques. *Corrosion Science*. 2015; 94:327-341. http://dx.doi.org/10.1016/j.corsci.2015.02.016.
5. Sathirachinda N, Pettersson R and Pan J. Depletion effects at phase boundaries in 2205 duplex stainless steel characterized with SKPFM and TEM/EDS. *Corrosion Science*. 2009; 51(8):1850-1860. http://dx.doi.org/10.1016/j.corsci.2009.05.012.
6. Tan H, Wang Z, Jiang Y, Han D, Hong J, Chen L, et al. Annealing temperature effect on the pitting corrosion resistance of plasma arc welded joints of duplex stainless steel UNS S32304 in 1.0 M NaCl. *Corrosion Science*. 2011; 53(6):2191-2200. http://dx.doi.org/10.1016/j.corsci.2011.02.041.
7. Chandra K, Singhal R, Kain V and Raja VS. Low temperature embrittlement of duplex stainless steel: Correlation between mechanical and electrochemical behavior. *Materials Science and Engineering*. 2010; 527(16-17):3904-3912. http://dx.doi.org/10.1016/j.msea.2010.02.069.
8. Číhal V. A potenciokinetic reactivation method for predicting the I.C.C. and I.G.S.C.C. sensitivity of stainless steels and alloys. *Corrosion Science*. 1980; 20(6):737-744. http://dx.doi.org/10.1016/0010-938X(80)90054-2.
9. Sedriks AJ. *Corrosion of stainless steels*. New York: John Wiley & Sons; 1979. 282 p.
10. Vijayalakshmi K, Muthupandi V and Jayachitra R. Influence of heat treatment on the microstructure, ultrasonic attenuation and hardness of SAF 2205 duplex stainless steel. *Materials Science and Engineering A*. 2011; 529:447-451. http://dx.doi.org/10.1016/j.msea.2011.09.059.
11. Guo LQ, Zhao XM, Li M, Zhang WJ, Bai Y and Qiao LJ. Annealing effects on the microstructure and magnetic domain structures of duplex stainless steel studied by in situ technique. *Applied Surface Science*. 2012; 259:213-218. http://dx.doi.org/10.1016/j.apsusc.2012.07.021.
12. Lara NO, Ruiz A, Rubio C, Ambriz RR and Medina A. Nondestructive assessing of the aging effects in 2205 duplex stainless steel using thermoelectric power. *NDT & E International*. 2011; 44(5):463-468. http://dx.doi.org/10.1016/j.ndteint.2011.04.007.
13. Zhang Z, Zhao H, Zhang H, Yu Z, Hu J, He L, et al. Effect of isothermal aging on the pitting corrosion resistance of UNS S82441 duplex stainless steel based on electrochemical detection. *Corrosion Science*. 2015; 93:120-125. http://dx.doi.org/10.1016/j.corsci.2015.01.014.
14. Calliari I, Zanesco M, Ramous E and Bassani P. Effects of Isothermal Ageing and Continuous Cooling after Solubilization in a Duplex Stainless Steel. *Journal of Materials Engineering and Performance*. 2007; 16(1):109-112. http://dx.doi.org/10.1007/s11665-006-9017-8.

15. Chen TH and Yang JR. Effects of solution treatment and continuous cooling on sigma-phase precipitation in a 2205 duplex stainless steel. *Materials Science and Engineering A*. 2001; 311(1-2):28-41. http://dx.doi.org/10.1016/S0921-5093(01)00911-X.
16. Cronemberger MER, Mariano NA, Coelho MFC, Pereira JN, Ramos ÉCT, de Mendonça R, et al. Study of cooling rate influence on SAF 2205 duplex stainless steel solution annealed. *Materials Science Forum*. 2014; 802:398-403. http://dx.doi.org/10.4028/www.scientific.net/MSF.802.398.
17. American Society for Testing and Materials - ASTM. *ASTM-E3-11: standard guide for preparation of metallographic specimens*. West Conshohocken; 2011.
18. American Society for Testing and Materials - ASTM. *ASTM-E407-07e1: standard practice for microetching metals and alloys*. West Conshohocken; 2007.
19. American Society for Testing and Materials - ASTM. *ASTM-G5-94: standard reference test method for making potentiostatic and potentiodynamic anodic polarization measurements*. West Conshohocken; 2011.
20. American Society for Testing and Materials - ASTM. *ASTM-D1141-98: standard practice for the preparation of substitute ocean water*. West Conshohocken; 2013.
21. Tait WS. *An introduction to electrochemical corrosion testing for practicing engineers and scientists*. Wisconsin: PairODocs Publishers; 1994.
22. Schultze S, Gollner J, Eick K, Veit P and Garz I. The modified EPR test: a new tool for examination of corrosion susceptibility of duplex stainless steel. In: *Proceedings of the International Conference on Duplex Stainless Steels 97*; 1997; Maastricht, The Netherlands. Zutphen: KCI Publishing; 1997. p. 639-648. Paper D97-067.
23. Rovere CAD, Santos FS, Silva R, Souza CAC and Kuri SE. Influence of long-term low-temperature aging on the microhardness and corrosion properties of duplex stainless steel. *Corrosion Science*. 2013; 68:84-90. http://dx.doi.org/10.1016/j.corsci.2012.10.038.
24. Číhal V and Stefec R. On the development of the electrochemical potentiokinetic method. *Electrochimica Acta*. 2001; 46(24-25):3867-3877. http://dx.doi.org/10.1016/S0013-4686(01)00674-0.
25. Man HC and Gabe DR. The determination of pitting potentials. *Corrosion Science*. 1981; 21(4):323-326. http://dx.doi.org/10.1016/0010-938X(81)90007-X.
26. Della Rovere CA, Aquino JM, Ribeiro CR, Silva R, Alcântara NG and Kuri SE. Corrosion behavior of radial friction welded supermartensitic stainless steel pipes. *Materials & Design*. 2015; 65:318-327. http://dx.doi.org/10.1016/j.matdes.2014.09.003.
27. Assis KS, Sousa FVV, Miranda M, Mattos ICPM, Vivier V and Mattos OR. Assessment of electrochemical methods used on corrosion of superduplex stainless steel. Corrosion Science. 2012; 59:71-80. http://dx.doi.org/10.1016/j.corsci.2012.02.014
28. Kim H-J, Jeon S-H, Kim S-T, Lee I-S, Park Y-S, Kim K-T, et al. Investigation of the sensitization and intergranular corrosion of tube-to-tubesheet welds of hyper duplex stainless steel using an electrochemical reactivation method. *Corrosion Science*. 2014; 87:60-70. http://dx.doi.org/10.1016/j.corsci.2014.06.005.
29. Pohl M, Storz O and Glogowski T. Effect of intermetallic precipitations on the properties of duplex stainless steel. *Materials Characterization*. 2007; 58(1):65-71. http://dx.doi.org/10.1016/j.matchar.2006.03.015.